

The Reaction of $\text{H}_8\text{Si}_8\text{O}_{12}$ with a Chromium Oxide Surface: A Model for Stainless Steel Surface Modification

J. N. Greeley,¹ S. Lee² and M. M. Banaszak Holl^{1*}

¹Chemistry Department, University of Michigan, Ann Arbor, MI 48109-1055, USA

²Chemistry Department, Brown University, Providence, RI 02912, USA

Many metal alloys are susceptible to corrosion, particularly after processing steps such as welding. Chemical vapor deposition (CVD) is an effective way to modify metal surfaces and impart specific physical and chemical properties. A hydrophobic, nanosegmented silicon oxide coating derived from the discrete cluster molecule $\text{H}_8\text{Si}_8\text{O}_{12}$ has been shown to chemisorb to 302 and 304 stainless steel. To understand better how this cluster binds to steel, a comprehensive study of these clusters adsorbed on chromium oxide was undertaken. IR, XPS and valence-band spectroscopies show convincingly that the clusters are chemisorbed intact on this surface. The coating also readily forms on molybdenum, tungsten, iron and nickel oxides, promising general application to a wide variety of metal alloys. Copyright © 1999 John Wiley & Sons, Ltd.

Keywords: silicon oxide; chromium oxide; chemical vapor deposition; chemisorption; spherosiloxane clusters

INTRODUCTION

Design and control of the surface properties of metals is critical for imparting desirable properties such as erosion and corrosion resistance while maintaining important bulk properties such as strength and ductility.^{1–3} Coatings of molecular thickness capable of providing protection over a wider range of potentials than the passive oxide

film of stainless steel could have significant technological impact. An important example of such surface modification involves the use of silicon, which forms a protective oxide coating on steels and inhibits oxidation, nitridation, erosion, corrosion and carbonization.^{4–12} The formation of a thin, adherent SiO_2 film, either by using silicon present in solid solution in the alloys or by depositing silicon on the surface from an SiH_4/H_2 mixture, has been vigorously pursued by Cabrera, Kirner and co-workers and is the basis of a commercial process.¹³ Deposition of silicon onto the surface avoids compromising the bulk steel properties, which can be impaired when too high a percentage of silicon is incorporated as part of an alloy composition. Another approach to the formation of SiO_2 films on surfaces has involved spherosiloxane clusters and resins. For example, the spherosiloxane cluster $\text{H}_8\text{Si}_8\text{O}_{12}$ (**1**) has been used as a chemical vapor deposition precursor for the generation of amorphous SiO_2 films.^{14,15} In addition, a considerable number of patents have been filed relating to protection of metals using silsesquioxane polymers.⁹ Indeed, much of the previous work in this area has been disclosed in the patent literature rather than in scientific journals; for examples, see Refs 16–20.

Coating steel surfaces with spherosiloxane clusters, molecules of the general formula $(\text{HSiO}_{1.5})_n$, such as $\text{H}_8\text{Si}_8\text{O}_{12}$,^{21–25} provides several advantages as a method for silicon oxide film formation. First, while silicon oxide surfaces are typically hydrophilic, the spherosiloxane clusters are intrinsically hydrophobic, yielding significantly different surface tribology. Second, the ambient-temperature gas-phase chemical vapor deposition (CVD) method described below generates a layer ~6 Å thick, making the process appropriate for application to microfabricated parts, samples with irregular morphologies or the insides of tubes. Third, the $\text{H}_8\text{Si}_8\text{O}_{12}$ clusters, composed entirely of eight-membered rings, are not porous, in contrast to

* Correspondence to: M. M. Banaszak Holl, Chemistry Department, University of Michigan, Ann Arbor, MI 48109-1055, USA. Contract/grant sponsor: National Science Foundation; Contract/grant number: DMR-9596208.

amorphous silicon oxide which is composed of a distribution of ring-sizes. Fourth, the spherosiloxane clusters are highly stable in acidic conditions; in fact they are made in the presence of either concentrated hydrochloric or sulfuric acid.^{21–23} Fifth, in contrast to a brittle α -SiO₂ layer, a film consisting of discrete spherosiloxane clusters contains many intercluster regions where the film can flex without breaking. Unlike the methods utilizing oxidation of silane and/or metal silicides, we are kinetically controlling the structure and content of the silicon oxide film, and therefore many of its key properties, by choice of cluster precursor (Klemperer *et al.* have made extensive use of the spherosiloxane cluster to control solid-state silicon oxide structure; lead references include Refs 24–26). Reported herein are initial results regarding the formation of nanosegmented, hydrophobic, ceramic silicon oxide films on a variety of the metal oxides that play a role in the passive layer of steels. Chromium oxide is highlighted because of the well-known correlation between the percentage chromium concentration at stainless steel grain boundaries and corrosion resistance.^{1–3}

EXPERIMENTAL

X-ray photoelectron spectroscopy (XPS) was performed using a PHI 5000C spectrometer and soft X-ray photoelectron spectroscopy (SXPS) was performed at beamline U8b at the National Synchrotron Light Source, Brookhaven National Laboratory. These facilities have been described previously.²⁷ Pure chromium oxide films were prepared on silicon wafers by sublimation from an ingot of chromium (99.998%) using a resistively heated tungsten basket, followed by oxidation using dioxygen (99.998%) or water. The films were judged to be clean of carbon and other impurities by XPS and were then exposed to 5×10^{-7} Torr of H₈Si₈O₁₂ at ambient temperature to form the spherosiloxane coating. All sample transfers were performed *in situ* in a system of ultrahigh-vacuum (UHV) chambers with a base pressure of better than 5×10^{-10} Torr. Nickel (99.9994%), iron (99.9975%), molybdenum (99.9%) and tungsten (99.95%) foils were obtained from Alfa-Aesar and converted to clean oxide surfaces by heating at 560 °C under 1×10^{-5} Torr oxygen. Two types of 0.125 mm stainless steel foils were used, SS-AISI T302 from Precision Brand and SS-AISI 304, Fe/Cr18/Ni10 from Goodfellow Corporation.

Spherosiloxane-coated samples of stainless steel were made by resistively heating the sample to approximately 560 °C under 1×10^{-5} Torr oxygen for 5 min to remove hydrocarbon contamination and provide an active surface for the binding of the clusters. The samples were then exposed to 5×10^{-7} Torr of H₈Si₈O₁₂ for 20 min at ambient temperature to form the spherosiloxane coating. This did not result in completely even heating and a temperature gradient typically existed of approximately 50 °C. Temperatures were routinely measured using a Minolta–Land infrared pyrometer (Cyclops 52, emissivity setting 0.4) that had been calibrated using a thermocouple directly attached to the steel sample and was accurate to $\pm 10\%$. Infrared spectroscopy was performed with a BioRad FTS-40 FTIR spectrometer, on samples in an UHV environment with the surface normal rotated 81° from the incident IR beam. Details of this experimental apparatus are described elsewhere.²⁸ Experiments typically involved taking a background spectrum, performing the desired CVD and then taking a second spectrum. The ratio of this second spectrum to the background was then calculated to arrive at the final plot. No other software manipulations were performed. All single-beam spectra represent a signal averaging of 256 scans taken with 8 cm⁻¹ resolution.

RESULTS AND DISCUSSION

Initial binding studies were performed on a chromium oxide surface with saturating doses of H₈Si₈O₁₂. Figure 1 shows the photoemission spectra observed for the Si 2*p* and O 1*s* core levels of the H₈Si₈O₁₂-modified chromium oxide surface. The 104 eV shift observed for the reaction of **1** with the chromium oxide surface is consistent with the presence of HSiO₃ and/or SiO₄ fragments. These structural moieties are known to have essentially identical binding energy (BE) shifts.²⁷ The O 1*s* core-level spectrum shows two distinct peaks. These are assigned as chromium oxide and H₈Si₈O₁₂-derived oxygens at 530.5 and 532.5 eV, respectively. Based upon the core-level shifts alone, we cannot strictly rule out cluster decomposition on the surface to form an amorphous siloxane network. However, soft X-ray photoemission studies of the valence-band region do provide additional evidence that the clusters have remained intact. Inspection of the Cr 2*p* core level shows an asymmetric shoulder on the high-BE side of the

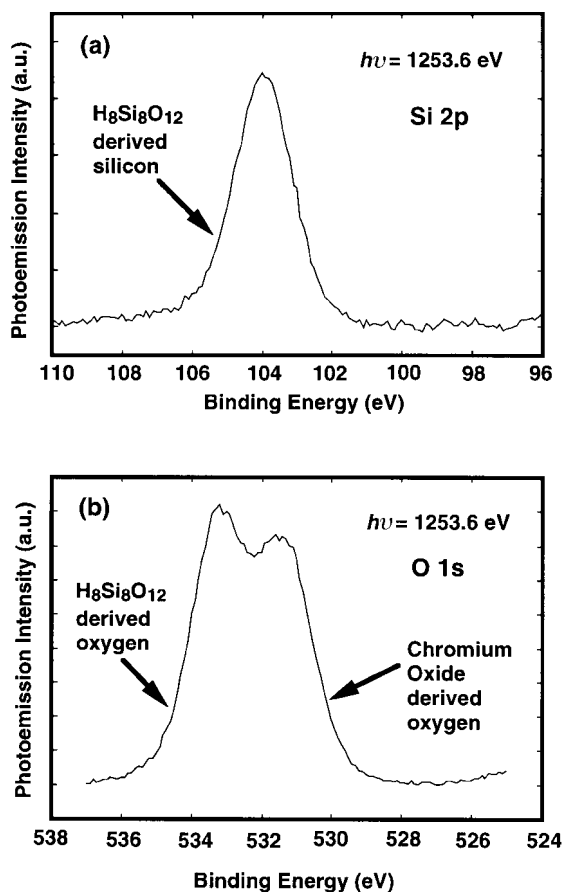


Figure 1 XPS spectra of (a) Si $2p$ and (b) O $1s$ core levels for the $\text{H}_8\text{Si}_8\text{O}_{12}$ -modified chromium oxide surface.

pure metal peak. The spectra can be nicely fitted with two peaks, one shifted roughly 3 eV higher than the known pure chromium metal BE. The shifted peak is assigned to chromium(III), most likely in the form Cr_2O_3 .²⁹

Valence-band (VB) spectra shown in Fig. 2 were obtained at the National Synchrotron Light Source, Brookhaven National Laboratory, in the following fashion. First, a chromium metal film was evaporated and oxidized. The valence-band spectrum of the chromium oxide film was then obtained using a photon energy of 170 eV (Fig. 2a, spectrum 1). The chromium oxide surface was then dosed with $\text{H}_8\text{Si}_8\text{O}_{12}$ and the VB spectrum taken again (Fig. 2a, spectrum 2). The convolution of the cluster-based valenceband features and the chromium-oxide-based valence-band features made it difficult to assess the structural fate of the clusters directly. However, by subtracting spectrum 1 from spectrum

2 the chromium oxide contribution can be effectively removed, leaving only the cluster-based contributions to the valence-band region. The effect of attenuation on the chromium oxide signals caused by the cluster overlayer was compensated for by setting the Cr $3d$ peak intensity equal for both spectra. The resulting cluster-derived valence-band features are shown in Fig. 2(b) spectrum 3, along with a series of comparison spectra. Note that for the intact, physisorbed clusters on Si(111)-H (Fig. 2b, spectrum 5), there are five readily discernible features in the valence-band region corresponding to the H-Si and Si-O bonding molecular orbitals. All of these features are maintained when 1 is chemisorbed by reaction of a single cluster Si-H bond with the surface dimers present on the Si(100) 2×1 surface, resulting in a symmetry reduction from O_h to C_{3v} (Fig. 2b, spectrum 4).²⁷ For the case of the cluster chemisorbed on the chromium oxide, features I and II are clearly still present and significant intensity is still present in regions III-V, although the features no longer stand out distinctly from one another. Spectrum 6 is from a film derived from $\text{H}_8\text{Si}_8\text{O}_{12}$ on Si(100) in which the cluster structure has been destroyed by heating and an amorphous hydrogen-containing siloxane network has been formed. Note that all the valence-band features associated with the high-symmetry $\text{H}_8\text{Si}_8\text{O}_{12}$ cluster are now gone. In fact, the valence band of this film is identical to amorphous SiO_2 . In summary, the valence-band spectra are consistent with the $\text{H}_8\text{Si}_8\text{O}_{12}$ clusters being largely, and possibly wholly, intact and bound via an Si-O linkage to the chromium oxide surface.

For a greater understanding of the binding geometry, reflection absorption infrared spectroscopy (RAIRS) was used. Surfaces were prepared by evaporating ~ 40 Å chromium (as judged by the attenuation of the Au $4f$ peaks) onto a gold surface. The RAIRS spectrum of a thin chromium oxide film on chromium is shown (Fig. 3, spectrum 1). A characteristic Cr-O stretch is observed at 1013 cm^{-1} . Exposure to a saturating dose of $\text{H}_8\text{Si}_8\text{O}_{12}$ clusters results in the observation of Si-H stretching and bending modes at 2283 and 889 cm^{-1} respectively. The cluster-derived Si-O stretch was observed at 1175 cm^{-1} . The RAIRS spectrum is consistent with intact discrete clusters as shown by Calzaferri *et al.* in solution,³⁰ and others on an Si(100) surface³¹. All of these features are consistent with the presence of HSiO_3 groups on the surface and the Si-O stretching frequency of 1175 cm^{-1} is indicative of intact spherosiloxane clusters and not amorphous SiO_2 .^{14,15} The single

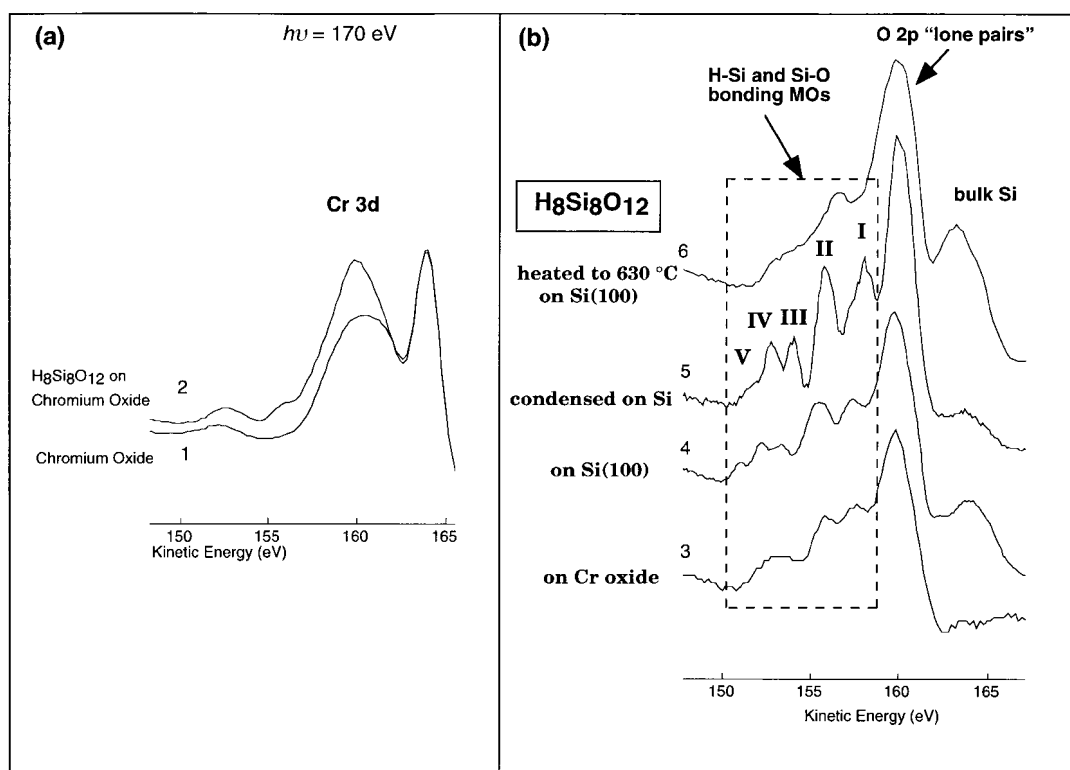


Figure 2 (a) Valence-band spectra of the $\text{H}_8\text{Si}_8\text{O}_{12}$ -modified chromium oxide (spectrum 2) and clean chromium surfaces (spectrum 1). (b) Spectrum 3 was obtained by subtracting spectrum 1 from spectrum 2. For comparison, $\text{H}_8\text{Si}_8\text{O}_{12}$ clusters chemisorbed on Si(100) (spectrum 4), physisorbed on Si(100) (spectrum 5) and thermally decomposed on Si(100) (spectrum 6) are shown.

peak is also inconsistent with amorphous networks of HSiO_3 fragments, which typically give a broad range of Si–O stretching frequencies varying from 1265 to 941 cm^{-1} .³¹

The sum total of the core-level XPS, valence-band and RAIRS data can be simply interpreted as the clusters bound via one or more silicon vertices to surface oxygen atoms. In principle, the Si–H bending mode can provide information on the symmetry of the bound cluster, and therefore the coordination mode to the surface. For example, the cluster modified at a single vertex reported by Calzaferri *et al.*, $\text{C}_6\text{H}_{13}(\text{H}_7\text{Si}_8\text{O}_{12})$, shows a distinct splitting of the single Si–H bending mode of the $\text{O}_h\text{-H}_8\text{Si}_8\text{O}_{12}$ cluster into three peaks.³⁰ Although the broadening we observe in the Si–H bending region is suggestive of such a change, the resolution and signal/noise ratio obtained in the RAIRS spectra do not allow any firm conclusions to be reached regarding the number of vertices activated. A possible structure of this adsorption geometry is shown in Fig. 4; however, it is important to

remember that we cannot distinguish this geometry from one that has two, three or four vertices bound to the surface.

It is worth noting that an alternative physisorption binding geometry was considered which involved a Lewis acid/Lewis base type of interaction between the cluster and the surface. It was proposed that one oxygen atom from the cluster (base) donated a lone pair into the acidic chromium(III). Both this model and the previously described chemisorption geometry are consistent with the XPS and RAIRS data. However, it can be seen in the VB spectra (Fig. 2b) that the chromium-oxide-modified surface (spectrum 3) does not contain many of the sharp spectral features observed for **1** physisorbed on a Si(100) surface (spectrum 5). Moreover, there is a strong correlation between the chromium-oxide-modified surface and **1** chemisorbed onto an Si(100) surface (spectrum 4). It is concluded, therefore, that the chemisorbed model best represents the binding geometry in this system.

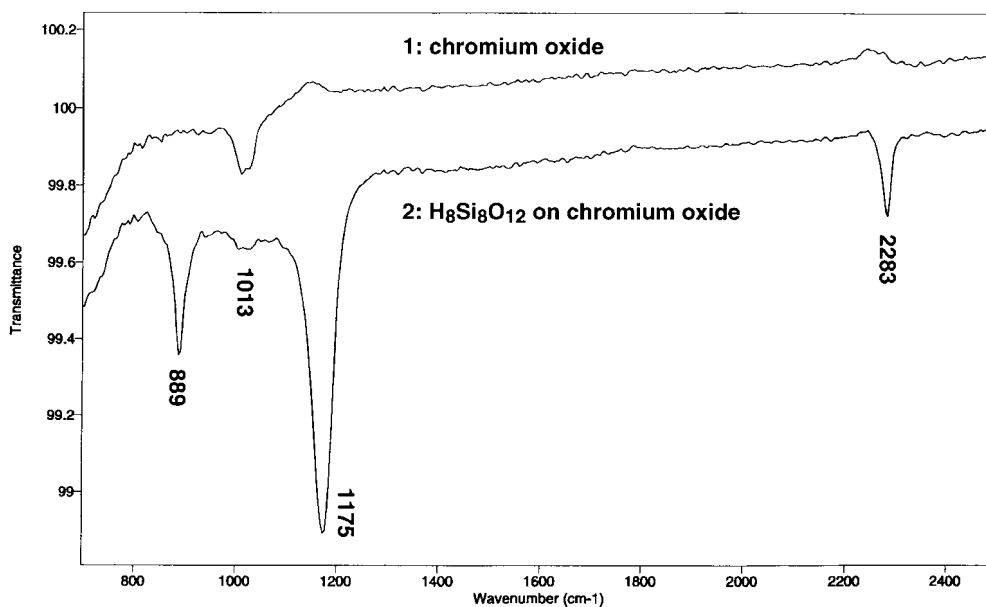


Figure 3 RAIRS spectrum of a thin chromium oxide film on chromium (spectrum 1), and $\text{H}_8\text{Si}_8\text{O}_{12}$ adsorbed on chromium oxide (2).

The reaction of the $\text{H}_8\text{Si}_8\text{O}_{12}$ cluster with iron, nickel, molybdenum and tungsten metal oxide films were also examined. These reactions were performed by oxidizing the pure metal foils in O_2 and exposing them to a saturating dose of $\text{H}_8\text{Si}_8\text{O}_{12}$ clusters. Although the absolute coverage of the clusters varied, the Si $2p$ core-level XPS data contained a single peak at 104 eV in all cases. This indicates that the cluster binding geometry on these metals is similar to that observed for the chromium oxide surface.

Stainless steels were also chosen as substrates.

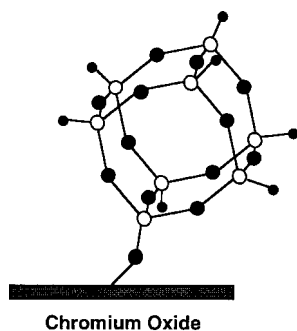


Figure 4 Proposed binding geometry for $\text{H}_8\text{Si}_8\text{O}_{12}$ chemisorbed via an oxygen atom to the chromium oxide surface.

The particular 302 and 304 stainless steels that we obtained were coated with a layer of organic material that persisted upon ultrasonic cleaning in a variety of solvents, preventing reaction with the cluster (Fig. 5a). However, heating the steel to 560°C under 1×10^{-5} Torr O_2 for 5 min significantly reduced the carbon content while greatly increasing the chromium oxide content at the surface (Fig. 5b). Note that an increase in iron and manganese oxides was also observed. Exposure of the activated steel surfaces to 5×10^{-7} Torr $\text{H}_8\text{Si}_8\text{O}_{12}$ clusters for 20 min resulted in spherosiloxane film formation on the steel surface (Fig. 5c). The cluster-based Si $2p$ and O $1s$ core levels are identical in terms of both binding energy shift and intensity to those observed on the pure chromium oxide surface. The 304 results are similar, although the Si $2p$ core-level region is more difficult to interpret because of the presence of amorphous SiO_2 , leading to overlapping spectral features. Once again, core-level XPS results were analogous to those obtained for chromium oxide. Analysis of the tungsten, and to a lesser extent nickel, oxides were complicated by adventitious silicon oxide films present on the foils when received. For these cases, observation of the O $1s$ core level was the most informative method. The $\text{H}_8\text{Si}_8\text{O}_{12}$ cluster reacts with a variety of metal oxide surfaces, including

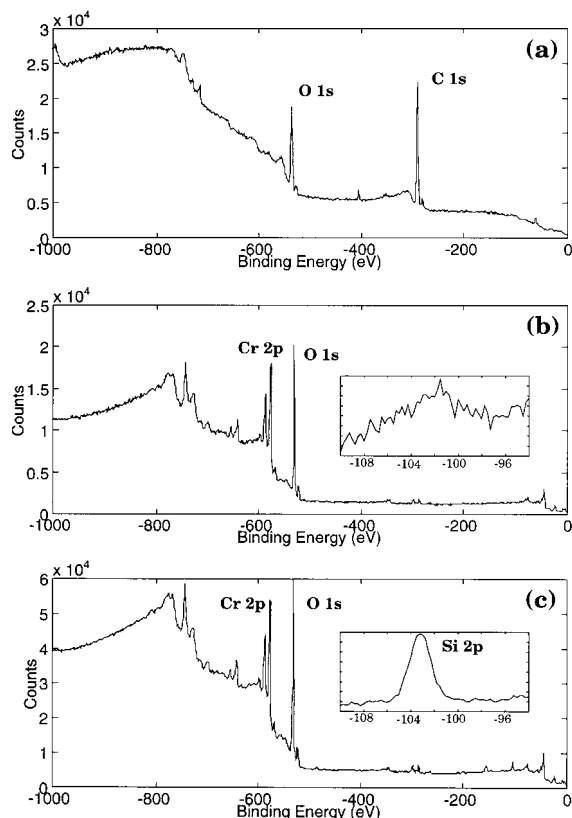


Figure 5 XPS spectra of 302 stainless steel (a) as received, (b) after oxidative treatment and (c) after exposure to $H_8Si_8O_{12}$. Inserts in (b) and (c) show higher-resolution scans of the Si 2p region.

heterogeneous surfaces such as stainless steel, depositing a roughly monolayer film of hydrophobic silicon oxide.

SUMMARY

A novel method for the formation of nanosegmented, hydrophobic silicon oxide films on a variety of metals oxide surfaces, including 302 and 304 stainless steels, has been demonstrated. Spectroscopic and chemical evidence indicate that the films consist of a single layer of chemisorbed $H_8Si_8O_{12}$ clusters bound to the metal or metal oxide surface by one or more linkages. In contrast to adventitious silicon oxide, sol-gel-based silicon oxide, and silicon oxide resulting from diffusion coatings,¹³ this coating approach provides an easily controlled self-limiting monolayer thickness of hydrophobic

silicon oxide. The chemical vapor deposition coating method makes this thin coating an interesting candidate for the protection of complex micromachined metal parts and tools.

Acknowledgements This work was supported by a grant from the National Science Foundation (DMR-9596208). Portions of this work were carried out at the National Synchrotron Light Source, Brookhaven National Laboratory, which is supported by the Department of Energy (Division of Materials Science and Division of Chemical Sciences). The authors thank C. L. Briant for his suggestions and encouragement.

REFERENCES

1. K. R. Trethewey and J. Chamberlain, *Corrosion for Science and Engineering*, 2nd edn, Longman Group, London, 1995.
2. R. Heitz, R. Henkhaus and A. Rahmel, *Corrosion Science: An Experimental Approach*, Ellis Horwood, New York, 1992.
3. C. L. Briant, *Metallurgical Aspects of Environmental Failures*, Elsevier, New York, 1985.
4. H. W. Grünling and R. Bauer, *Thin Solid Films* **95**, 3 (1982).
5. L. H. Dubois and R. G. Nuzzo, *J. Vac. Sci. Technol. A* **2**, 441 (1984).
6. A. L. Cabrera, J. F. Kirner and J. N. Armor, *J. Mater. Res.* **6**, 71 (1991).
7. A. L. Cabrera, J. F. Kirner and R. Pierantozzi, *J. Mater. Res.* **5**, 74 (1990).
8. A. L. Cabrera and J. F. Kirner, *Chemtech* **19**, 558 (1989).
9. A. L. Cabrera, E. J. Karwacki and J. F. Kirner, *Appl. Surf. Sci.* **1988**, **32**, 239 (1988).
10. J. F. Kirner, M. R. Anewalt, E. J. Karwacki and A. L. Cabrera, *Metal. Trans. A* **19**, 3045 (1988).
11. B. Le Dinh Boa and I. Ignatiadis, *Mater. Sci. Forum* **126-128**, 663 (1993).
12. J. Liu, H. Tomioka, L. Arnberg and S. J. Savage, *Mater. Lett.* **8**, 381 (1989).
13. A. L. Cabrera, J. F. Kirner, R. A. Miller and R. Pierantozzi, US Patent 4714632 (1987).
14. S. B. Desu, C. H. Peng, T. Shi and P. A. Agaskar, *J. Electrochem. Soc.* **139**, 2682 (1992).
15. M. D. Nyman, S. B. Desu and C. H. Peng, *Chem. Mater.* **5**, 1636 (1993).
16. W. T. Collins and C. L. Frye, US Patent 3615272 (1971).
17. L. F. Hanneman, T. E. Gentle and K. G. Sharp, US Patent 5118530 (1992).
18. T. E. Gentle, US Patent 5279661 (1994).
19. M. N. Eckstein and D. S. Ballance, US Patent 5310583 (1994).
20. K. Mine, T. Nakamura and M. Sasaki, US Patent 5372842 (1994).
21. P. Agaskar, *Inorg. Chem.* **30**, 2707 (1991).
22. C. L. Frye and W. T. Collins, *J. Am. Chem. Soc.* **92**, 5586 (1970).

23. R. Müller, R. Kohne and S. Sliwinski, *J. Prakt. Chem.* **9**, 71 (1959).
24. C. S. Brevett, P. C. Cagle, W. G. Klemperer, D. M. Millar and G. C. Ruben, *J. Inorg. Organometal Polym.* **1**, 335 (1991).
25. P. C. Cagle, W. G. Klemperer and C. A. Simmons, *Mater. Res. Soc. Proc. Symp.* **180**, 29 (1990).
26. W. G. Klemperer, V. V. Mainz and D. M. Millar, *Mater. Res. Soc. Proc. Symp.* **73**, 3 (1986).
27. S. Lee, S. Mekan, M. M. Banaszak Holl and F. R. McFeely, *J. Am. Chem. Soc.* **116**, 11819 (1994) and references therein.
28. J. N. Greeley, L. M. Meevwenberg and M. M. Banaszak Holl, *J. Am. Chem. Soc.* **120**, 7776 (1998).
29. C. Palacio, H. J. Mathieu and D. Landolt, *Surf. Sci.* **182**, 41 (1987).
30. G. Calzaferri, R. Imhof and K. W. Törnroos, *J. Chem. Soc., Dalton Trans.* 3123 (1994).
31. J. Eng, K. Ragavachari, L. M. Struck, Y. J. Chabal, B. E. Bent, M. M. Banaszak Holl, F. R. McFeely, A. M. Michaels, G. W. Flynn, S. B. Christman, E. E. Chaban, G. P. Williams, K. Radermacher and S. Mantl, *J. Chem. Phys.* **108**, 8680 (1998).
32. FTIR Analysis of FOx[®] Flowable Oxide Thin Film, Dow-Corning Technical Note.